REGOLITH CHARACTERIZATION USING LROC NAC DIGITAL ELEVATION MODELS OF SMALL LUNAR CRATERS. J. D. Stopar[1], M. S. Robinson[1], E. J. Speyerer[1], K. Burns[1], H. Gengl[1], and the LROC Team.
[1] School of Earth and Space Exploration, Arizona State University, Tempe, AZ (jstopar@asu.edu).

Introduction: Characterization of the lunar regolith is important for future surface activities and is one of the primary goals of the Lunar Reconnaissance Orbiter Camera (LROC) [1]. The ~0.5 m/pixel scale images of the Narrow Angle Cameras (NAC) allow investigation of regolith structure and properties. Digital Elevation Models (DEMs) created from available stereo NAC pairs provide topography of small craters (30m<D<300m) whose shapes may be influenced by regolith properties. Morphologies of small craters provide important insight into the structure and thickness of the regolith due to the relationship between crater shape and changes in material strength between subsurface layers [e.g., 2-3] and/or differential degradation rates [e.g., 4-6]. The morphometry of small craters may also reflect their origin as primary or secondary impacts and has important implications for the determination of the recent impact rate and age dating techniques [e.g., 7-8]. NAC images and derived DEM products provide morphometric data for large populations of small craters across all lunar terrains. Such observations are used to assess distribution and frequency of secondary craters as well as morphologic variability of small craters due to terrain and degradation. To investigate relationships among crater shape, origin (i.e., secondary vs primary), age, and target, we extracted profiles, depths, diameters, and slopes from more than 850 small craters in mare and non-mare terrains.

Methods: Study regions were selected to represent a range of lunar terrain types and ages, but also correspond to the current availability of NAC DEMs. Sites and craters are summarized in Table 1. "Herringbone-pattern", clustered, and irregularly shaped secondaries were excluded; however, circular secondaries may be included due to the difficulty of distinguishing them from small primary craters.

Crater degradation was determined following [4] where fresh "A" craters have crisp rims, visible ejecta rays, and no superposed craters. "AB" craters have distinct rims and some visible ejecta rays. "B" craters are more degraded but still have distinct rims although rays have faded. Craters degraded beyond this state are not included at this time, but will be included in future analysis. Crater profiles, depths, and rim-to-rim diameters were determined from 16 NAC DEMs. The DEMs were created using the methods of [9] with 2-m post spacing and reported precisions better than 3m when registered to LOLA elevation tracks (Table 1). To provide confidence in measurements determined from the DEM profiles, for D>100m, profiles were compared to LOLA tracks when a track crossed through the center of the crater (rare). There is general agreement between depths of craters in NAC DEMs and LOLA profiles; however, further work is needed to confirm the accuracy of depth measurements of small craters.

Slopes, d/D ratios, and circularity (D_2/D_1) were determined from topographic profiles. Craters on slopes >12° were excluded if the shape of the crater was affected such that one rim is significantly higher than the other or the crater is strongly asymmetric. Relative standard deviations (RSDs) of crater slopes were calculated as a percentage given by: RSD[dz/dx] = 100 × standard_deviation/average.

TABLE 1: Summary of sites and craters.

Site	Center Lat/Lon	Terrain	DEM precision (m)	Area (km^2)	A Craters (n)	AB Craters (n)	B Craters (n)	Sum Craters (n)	Craters/km^2
Apollo15	26.1°, 3.5°E	mixed	1.06	145.9	7	5	20	32	0.22
Bhabha	54.6°, 161.5°E	non-mare	2.68	173.0	4	10	11	25	0.14
Hortensius	7.6°, 332.2°E	mare	0.86	135.2	6	3	57	66	0.49
Ina	18.5°, 5.3°E	mixed	1.07	120.9	4	6	51	61	0.50
Luna24	12.6°, 62.2°E	mare	1.01	149.3	4	75	110	189	1.27
Marius	13.7°, 303.9°E	mare							
M111			0.95	129.7	1	4	12	17	0.13
M137			0.91	132.9	1	13	18	32	0.24
M144			0.85	141.6	1	9	29	39	0.28
Orientale	11.8°, 237.8°E	non-mare	0.95	147.8	6	11	29	46	0.31
Ranger6	9.2°, 21.5°E	mare	0.9	131.8	4	14	28	46	0.35
Reiner Gamma	7.4°, 301.5°E	mare							
M129			0.82	123.2	5	14	62	81	0.66
M135			0.91	139.7	3	19	53	75	0.54
M145			0.89	149.7	3	21	55	79	0.53
SPA	50.9°, 171.2°E	non-mare							
M123			1.98	171.4	1	5	17	23	0.13
M138			2.72	222.2	3	8	26	37	0.17
M141			2.67	222.6	2	10	26	38	0.17

Results: *Profile Shape.* Craters with V-shaped profiles are characterized by steep walls and little to no floor; U-shaped craters have a larger, often flat, floor and frequently have breaks in slope on the walls. Craters with larger floors have high RSDs, typically >80%, while V-shaped profiles have low RSDs, typically <65%. Other crater morphologies can have a range of RSDs representing the relative variations in crater wall slopes. Fig. 1 shows a sequence of progressively larger craters in the Ranger 6 mare terrain that transition from V-shaped to U-shaped with increasing crater diameter due to a coherent or consolidated layer at depth.

d/D and Terrain. No strong correlations between terrain type and d/D ratios were observed, with a few minor exceptions (Fig. 2). For example, Luna 24 and Reiner Gamma appear to have a larger number of craters with d/D ~0.1. However, these sites also have a larger number of total craters. Possible factors include a higher abundance of secondaries, different crater populations, or, perhaps, the lighting conditions were more favorable for identification of small craters at these sites. Fig. 2 (table) summarizes the linear trends in d/D for each site. All sites have best-fit d/D ratios between 0.11 and 0.15. The average d/D for all craters is 0.11±0.03; for D≥50m, d/D_{avg}=0.12±0.02; and for D≥100m, d/D_{avg}=0.13±0.03.

FIG. 1: Four fresh craters in Ranger6 mare terrain with increasing crater diameter (left to right: 34m, 47m, 50m, 62m) and area of floor material.

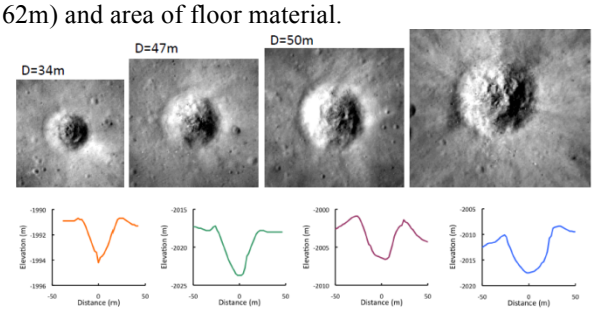

FIG. 2: d/D for each terrain. Upper dashed line is d/D=0.2; lower dashed line is d/D=0.1; D_{circ}=craters with circularity 0.95-1.05

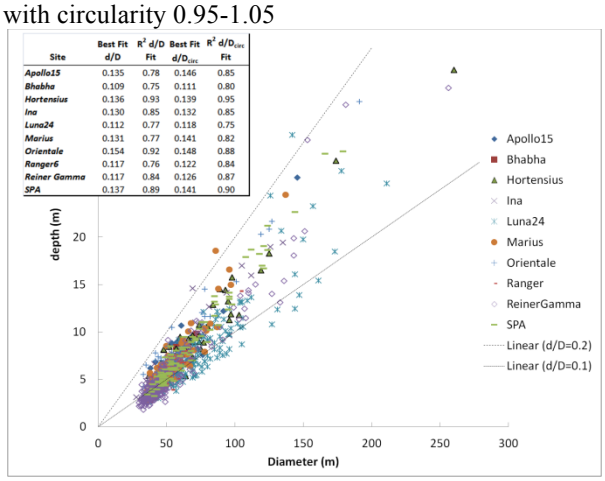

Site	Best Fit d/D	R^2 d/D Fit	Best Fit d/D_{circ}	R^2 d/D_{circ} Fit
Apollo15	0.135	0.78	0.146	0.85
Bhabha	0.109	0.75	0.111	0.80
Hortensius	0.136	0.93	0.139	0.95
Ina	0.130	0.85	0.132	0.85
Luna24	0.112	0.77	0.118	0.75
Marius	0.131	0.77	0.141	0.82
Orientale	0.154	0.92	0.148	0.88
Ranger6	0.117	0.76	0.122	0.84
Reiner Gamma	0.117	0.84	0.126	0.87
SPA	0.137	0.89	0.141	0.90

Discussion: *d/D and Degradation.* Previous workers [4,10] suggested that d/D of craters decrease as they degrade due to infilling of the floor and erosion of the crater rim. In this analysis, however, no trend was observed between d/D and degradation states A, AB, and B. This discrepancy is best explained by the exclusion of heavily degraded craters and/or the scarcity of fresh "A" craters (only 6% of the included craters). Other factors may include a high percentage of secondary craters, inaccuracies in depths of small craters derived from NAC DEMs, or differences in how crater degradation state was determined between this study and [4]. Further analysis of more degraded craters is yet needed.

Maximum Slopes. A positive linear correlation was observed between increasing maximum slope within the crater and increasing crater diameter. This trend is consistent with the reduced ability of small craters to penetrate the upper unconsolidated regolith into coherent materials at depth. This correlation is also consistent with large blocks and benches occurring more often in larger craters.

Secondary Craters. Only 2 of the more than 850 craters (<<1%) have d/D ≥0.2. If d/D=0.2-0.3 defines primary simple craters [e.g., 4,11-12], then the craters in this study are nearly all secondaries (even though all obvious secondaries were excluded). Some authors have suggested that most craters D<1 km are likely to be secondary craters [e.g., 7-8,13]. Given the freshness of the craters in this study, degradation does not explain the low d/D ratios. However, we observed a positive correlation between decreased crater diameter and decreasing circularity, suggesting that at least 40% of the studied crater population with circularities ~0.9 and 1.1 may indeed be secondary craters. Fig. 2 (table) shows best-fit d/D ratios for each site when craters with circularity <0.95 and >1.05 are excluded. In most cases, the error of the fit is improved; however, even circular craters have d/D <0.2. These preliminary results suggest that circularity may be a non-unique criterion for distinguishing between primary and secondary craters.

Conclusions: For craters 30<D<300 m in diameter, our results indicate that profile shapes vary with local regolith properties, slope, degradation state, and geologic unit as suggested by the complex history and nature of the regolith and are generally consistent with previous works [2,4,14-15]. In the mare, a greater number of flat-floored craters were observed, suggesting consolidated materials are found closer to the surface in these terrains, consistent with a thinner regolith layer [e.g., 2,16]. However, there are exceptions to these trends in both mare and non-mare terrains due to local variations in regolith and subsurface structure, consistent with [e.g., 2,14]. Our preliminary analysis shows that most craters D<300m have d/D ratios <0.2, implying that most craters in this size range are shallow and possibly secondaries rather than primaries. However, further work is needed to confirm these results by including more degraded craters in the study, a detailed assessment of the accuracy of depths determined from NAC DEMs (including minimum D for accurate depth measurements), and a survey of d/Ds for known secondary crater populations to better characterize secondary populations in different terrains.

References: [1] Robinson et al. (2010) SSR 150:81-124. [2] Quaide and Oberbeck (1968) JGR 73:5247-5270. [3] Young et al. (1974) Proc. LPSC 5th, p.159-170. [4]Basilevsky (1976) Proc. LPSC 7th, p.1005-1020. [5]Schultz et al. (1977) Proc. LPSC 8th, p.3539-3564. [6] Oberbeck (1975) Rev. Geophys. Space Phys. 13:337-362. [7] Pike and Wilhelms (1978) LPSC 9th, p.907-909. [8] McEwen and Bierhaus (2006) Annu. Rev. Earth Planet. Sci. 34:535-567. [9] Tran et al. (2010) LPSC 41 #2515. [10]Soderblom and Lebofsky (1972) JGR 77:279-296. [11] Pike (1974) GRL 1:291-294. [12] Pike (1977) Proc. LPSC 8th, p.3427-3436. [13] Shoemaker (1962) in Phys. And Astron. Of the Moon p.283-359. [14] Wilcox et al. (2005) MAPS 40:695-710. [15] Mizutani et al. (1983) Proc LPSC 13th, p. 835-845. [16] Bart et al. (2011) LPSC 42 #2597.